



# Mitochondrial Atpif1 regulates heme synthesis in developing erythroblasts

## Citation

Shah, Dhvanit I., Naoko Takahashi-Makise, Jeffrey D. Cooney, Liangtao Li, Iman J. Schultz, Eric L. Pierce, Anupama Narla, et al. 2012. Mitochondrial atpif1 regulates heme synthesis in developing erythroblasts. *Nature* 491(7425): 608-612.

## Published Version

doi:10.1038/nature11536

## Permanent link

<http://nrs.harvard.edu/urn-3:HUL.InstRepos:11179038>

## Terms of Use

This article was downloaded from Harvard University's DASH repository, and is made available under the terms and conditions applicable to Other Posted Material, as set forth at <http://nrs.harvard.edu/urn-3:HUL.InstRepos:dash.current.terms-of-use#LAA>

## Share Your Story

The Harvard community has made this article openly available.  
Please share how this access benefits you. [Submit a story](#).

[Accessibility](#)

Published in final edited form as:

*Nature*. 2012 November 22; 491(7425): 608–612. doi:10.1038/nature11536.

## Mitochondrial Atpif1 regulates heme synthesis in developing erythroblasts

Dhvanit I. Shah<sup>1</sup>, Naoko Takahashi-Makise<sup>2</sup>, Jeffrey D. Cooney<sup>1,†</sup>, Liangtao Li<sup>2</sup>, Iman J. Schultz<sup>1,†</sup>, Eric L. Pierce<sup>1</sup>, Anupama Narla<sup>1,3</sup>, Alexandra Seguin<sup>2</sup>, Shilpa M. Hattangadi<sup>3,4</sup>, Amy E. Medlock<sup>5</sup>, Nathaniel B. Langer<sup>1,†</sup>, Tamara A. Dailey<sup>5</sup>, Slater N. Hurst<sup>1</sup>, Danilo Faccenda<sup>6</sup>, Jessica M. Wiwczar<sup>7,†</sup>, Spencer K. Heggers<sup>1</sup>, Guillaume Vogin<sup>1,†</sup>, Wen Chen<sup>1,†</sup>, Caiyong Chen<sup>1</sup>, Dean R. Campagna<sup>8</sup>, Carlo Brugnara<sup>9</sup>, Yi Zhou<sup>3</sup>, Benjamin L. Ebert<sup>1</sup>, Nika N. Danial<sup>7</sup>, Mark D. Fleming<sup>8</sup>, Diane M. Ward<sup>2</sup>, Michelangelo Campanella<sup>6</sup>, Harry A. Dailey<sup>5,\*</sup>, Jerry Kaplan<sup>2,\*</sup>, and Barry H. Paw<sup>1,3,\*</sup>

<sup>1</sup>Department of Medicine, Division of Hematology, Brigham and Women's Hospital, Harvard Medical School, Boston, Massachusetts 02115, USA

<sup>2</sup>Department of Pathology, University of Utah School of Medicine, Salt Lake City, Utah 84312, USA

<sup>3</sup>Department of Medicine, Division of Hematology-Oncology, Boston Children's Hospital, Harvard Medical School, Boston, Massachusetts 02115, USA

<sup>4</sup>Whitehead Institute for Biomedical Research and Massachusetts Institute of Technology, Cambridge, Massachusetts 02142, USA

<sup>5</sup>Biomedical and Health Sciences Institute, Departments of Microbiology, Biochemistry & Molecular Biology, University of Georgia, Athens, Georgia 30602, USA

<sup>6</sup>Royal Veterinary College, University of London and University College London Consortium for Mitochondrial Research, London, NW1 0TU, UK

<sup>7</sup>Department of Cancer Biology, Dana-Farber Cancer Institute, Harvard Medical School, Boston, Massachusetts 02115, USA

\*Addresses for correspondence: B.H.P., bpaw@rics.bwh.harvard.edu; H.A.D., hdailey@uga.edu; J.K., jerry.kaplan@path.utah.edu.

†Present addresses: University of Texas Health Science Center, San Antonio, Texas, USA (J.D.C.); InteRNA Technologies, Utrecht, The Netherlands (I.J.S.); Columbia University, New York, New York, USA (N.B.L.); Texas A&M Health Science Center, Temple, Texas, USA (W.C.); Yale University, New Haven, CT, USA (J.M.W.); Alexis Vautrin Cancer Center, Vandoeuvre-Les-Nancy, France (G.V.).

**Full Methods** and any associated references are available in the online version of the paper at [www.nature.com/nature](http://www.nature.com/nature).

Supplementary Information is linked to the online version of the paper at [www.nature.com/nature](http://www.nature.com/nature).

**GenBank accession numbers.** Sequences are available in GenBank as follows: Zebrafish *atpif1a* (NM\_001089521.1), zebrafish *atpif1b* (NM\_001044859), mouse *Atpif1* (NC\_000070.5), and human *ATPIF1* (NC\_005104.2). Reprints and permissions information is available at [npg.nature.com/reprints](http://npg.nature.com/reprints) and permissions.

**Author Contributions.** D.I.S. and B.H.P. originally conceived the project, designed and performed the experiments, analyzed data, and wrote the manuscript. N.T.M., A.S., L.L., D.M.W., and J.K. measured <sup>59</sup>Fe uptake in mitochondria and complexed in heme, PPIX levels, Fech activity, xanthine oxidase and aconitase activities, and heme levels in yeast knock-out for *Inh1*, and participated in scientific discussions. J.D.C., I.J.S., E.L.P., and N.L.B. did microinjections in zebrafish embryos. S.K.H., G.V., C.C., and W.C. helped with zebrafish colony maintenance and protein experiments. Y.Z. helped with high resolution meiotic mapping. A.N., S.N.H., and B.L.E. helped with silencing *ATPIF1* in human primary CD34+ cells. S.M.H. helped with silencing *Atpif1* in MFPL cells. A.E.M., T.A.D., and H.A.D. created Fech constructs for injection, measured Fech activity as a function of pH, Fech activity, analyzed Fech structure for [2Fe-2S] clusters, and participated in scientific discussions. D.F., J.M.W., M.C. and N.N.D. helped to design and measure mitochondrial physiological parameters. C.B. analyzed *pnt* adult blood parameters. D.C. and M.D.F. helped with electron microscopic analysis of mitochondrial structure and disease.

**Author Information** The authors declare no competing financial interests

<sup>8</sup>Department of Pathology, Boston Children's Hospital, Harvard Medical School, Boston Massachusetts 02115, USA

<sup>9</sup>Department of Laboratory Medicine, Boston Children's Hospital, Harvard Medical School, Boston, Massachusetts 02115, USA

## SUMMARY

Defects in the availability of heme substrates or the catalytic activity of the terminal enzyme in heme biosynthesis, ferrochelatase (Fech), impair heme synthesis, and thus cause human congenital anemias<sup>1,2</sup>. The inter-dependent functions of regulators of mitochondrial homeostasis and enzymes responsible for heme synthesis are largely unknown. To uncover this unmet need, we utilized zebrafish genetic screens and cloned mitochondrial *ATPase inhibitory factor 1* (*atpif1*) from a zebrafish mutant with profound anemia, *pinotage* (*pnt*<sup>*tq209*</sup>). We now report a direct mechanism establishing that Atpif1 regulates the catalytic efficiency of vertebrate Fech to synthesize heme. The loss of *Atpif1* impairs hemoglobin synthesis in zebrafish, mouse, and human hematopoietic models as a consequence of diminished Fech activity, and elevated mitochondrial pH. To understand the relationship among mitochondrial pH, redox potential, [2Fe-2S] clusters, and Fech activity, we used (1) genetic complementation studies of Fech constructs with or without [2Fe-2S] clusters in *pnt*, and (2) pharmacological agents modulating mitochondrial pH and redox potential. The presence of [2Fe-2S] cluster renders vertebrate Fech vulnerable to Atpif1-regulated mitochondrial pH and redox potential perturbations. Therefore, *Atpif1* deficiency reduces the efficiency of vertebrate Fech to synthesize heme, resulting in anemia. The novel mechanism of Atpif1 as a regulator of heme synthesis advances the understanding of mitochondrial heme homeostasis and red blood cell development. A deficiency of *Atpif1* may contribute to important human diseases, such as congenital sideroblastic anemias and mitochondriopathies.

---

A deficiency in heme, which is used in a wide variety of metabolic and regulatory pathways in cells<sup>3</sup>, results in pathological conditions that range from mild anemia to early *in utero* death<sup>4</sup>. As an essential component of hemoglobin, the individual enzymes and substrates of heme biosynthesis have been well studied<sup>2</sup>; however, key gaps remain in our knowledge of genes that regulate iron and heme trafficking and homeostasis. This incomplete understanding prevents researchers from developing targeted therapies for a broad range of disorders, including congenital anemias and porphyrias, as well as metabolic and neurological disorders.

We recovered *pnt*, a zebrafish non-lethal recessive mutant, from an unbiased ethyl nitrosourea (ENU) mutagenesis screen<sup>5</sup> for defects in circulating erythroid cells<sup>6</sup>. *pnt* embryos were anemic (Fig. 1a) despite normal expression of erythroid cell markers,  $\beta$ -globin and band-3 (data not shown). Based on red cell indices, the erythrocytes from *pnt* embryos that survive to adult stage exhibited hypochromic, microcytic anemia (Supplementary Fig. 1a). Histological analysis of adult *pnt* hematopoietic tissues, showed no gross morphological defects (Supplementary Fig. 1b).

The positional cloning and chromosomal walk identified the most telomeric gene, the mitochondrial *ATPase inhibitory factor 1* (*atpif1a*; *zgc:162207*), as the most likely candidate for the *pnt* locus (Fig. 1b). Phylogenetic analysis showed that an *ATPase inhibitory factor 1-like protein* (*atpif1b*; *zgc: 153321*) on Chr. 17 is 71% similar to *atpif1a* at the amino acid level (Fig. 1d), and is likely the result of gene duplication in teleosts<sup>7</sup>. Peptide alignments further displayed human (*ATPIF1*, chromosome 1) and mouse (*Atpif1*, chromosome 4) homologs for *atpif1a* and *atpif1b* (Fig. 1c). Quantitative reverse transcriptase-polymerase chain reaction (qRT-PCR) showed reduced levels of *atpif1a* mRNA in *pnt* embryos (Fig. 1d) and *pnt* adult kidney marrow compared to respective wild-type (WT) controls

(Supplementary Fig. 1c). The levels of *atpif1b* mRNA were, however, unchanged in *pnt* embryos (Fig. 1d) and elevated 2 to 3-fold in *pnt* adult kidney marrow (Supplementary Fig. 1c). Thus, *atpif1a* is likely the gene disrupted in the *pnt* locus. Previous studies have shown that mitochondrial *Atpif1* regulates the proton motive force via mitochondrial influx of H<sup>+</sup> ions, mitochondrial structure, and ATP synthesis, indicating that *Atpif1* is required in a wide range of metabolically active tissues<sup>8</sup>. The broad requirement for *Atpif1* is reinforced by the ubiquitous expression of both *atpif1a* and *atpif1b* in zebrafish embryos (Supplementary Fig. 1d), and *Atpif1* in various mouse adult and fetal organs (Supplementary Fig. 1e).

To verify the loss-of-function phenotype for *atpif1a*, we injected two *atpif1a* antisense morpholinos (MO), a splice-blocking (Fig. 2a) and a translational-blocking (data not shown), to knock down *atpif1a* expression in zebrafish embryos. The *atpif1a*-silenced embryos (morphants) lacked hemoglobinized cells, as detected by *o*-dianisidine staining, thereby phenocopying the anemia in *pnt* embryos (Fig. 2a). The anemic phenotype in the morphant embryos correlates with a reduction of *atpif1a* mRNA levels, verifying that the splice-blocking MO accurately targeted *atpif1a* (Fig. 2b, Supplementary Discussion 1, Supplementary Figs. 2a–2d).

To further validate that *atpif1a* is the gene disrupted in *pnt*, we over-expressed *atpif1a* cRNA in *pnt* embryos and subsequently evaluated their hemoglobinization. To assess the specificity of our complementation assay, we also injected *pnt* embryos with non-functional *atpif1a* cRNA harboring a mis-sense mutation (E26A) in the regulatory inhibitory domain<sup>9</sup>. Only functional *atpif1a* complemented the anemia in *pnt* embryos (Fig. 2c), thereby confirming that *atpif1a* is the gene disrupted in *pnt* embryos. Consistent with 2 to 3-fold increase in *atpif1b* expression in surviving *pnt* adults (Supplementary Fig. 1c), the ectopic-expression of *atpif1b* cRNA also complemented *pnt* anemia (Fig. 2c), a result of their redundant function. These data suggest that the hypomorphic and viable phenotype of *pnt* could be attributed to the ability of *atpif1b* to partially compensate for the loss of function of *atpif1a* (Supplementary Fig. 1c). This is in contrast to other situations with paralogous genes such as the *mitoferrin* (*mfrn*) transporters<sup>10</sup>.

To identify a genetic mutation in the *pnt* locus, we first sequenced the open reading frame (ORF) and splice junctions of the *atpif1a* gene and found no mutation. Instead, a polymorphism in the 3' untranslated region (UTR) of the *atpif1a* gene was discovered (Fig. 2d). This mutation was linked to the *pnt* locus following the distinct segregation of WT and mutant (MT) conformations on single-strand conformational polymorphism (SSCP) (Fig. 2e). To establish the functional consequences of the 3'UTR polymorphism on the stability of *atpif1a* mRNA, we designed constructs containing the zebrafish *atpif1a* ORF fused with either the WT or polymorphic 3'UTR sequences, and transfected mouse erythroleukemia (MEL) cells with each construct individually for stable selection (Supplementary Fig. 2e). qRT-PCR analysis showed a decrease in steady state *atpif1a* mRNA levels in cells harboring polymorphic 3'UTR constructs as compared to the WT construct (Fig. 2f, Supplementary Discussion 2). These data functionally demonstrate that the polymorphism in the 3'UTR of the *atpif1a* gene destabilizes its steady state mRNA. The observed decrease in the *atpif1a* mRNA level in *pnt* embryos (Fig. 1d) is consistent with the ascribed function for the 3'UTR polymorphism, which destabilizes *atpif1a* steady state mRNA and leads to its degradation<sup>11</sup>.

In mammalian cells, *Atpif1* is located in the inner mitochondrial membrane and primarily regulates the function of the F<sub>1</sub>F<sub>0</sub>-ATP synthase<sup>12</sup>. There is, however, no direct evidence suggesting a role for *Atpif1* in heme synthesis or erythropoiesis. To ascertain the role of *Atpif1* in mammalian heme synthesis, we utilized short hairpin RNAs (shRNAs) to stably silence *Atpif1* in differentiating mammalian erythroid cells: human primary CD34+

(hCD34+) cells, mouse primary fetal liver (MPFL), and MEL cells. The reduced number of hemoglobinized cells in *Atpif1*-silenced hCD34+ and MEL cells (Fig. 3a, Supplementary Fig. 3a) and the reduced hemoglobin content in MPFL cells transduced with *Atpif1*-shRNAs (Supplementary Figs. 3b–3c), demonstrate conserved heme-specific function of Atpif1. Consistent with a high turnover of heme in developing erythroblasts<sup>13</sup>, we observed that the hemoglobinization defect was specific to *Atpif1*-silenced differentiating erythroid cells. Similarly, we observed that the expression of Atpif1 protein increases along with other proteins required for heme synthesis<sup>14</sup>, such as Fech and mitoferrin1 (*Mfn1*, *Slc25a37*), during terminal erythroid maturation (Supplementary Fig. 3d). Analogous *Atpif1*-silencing experiments performed in non-erythroid (NIH3T3) and undifferentiated MEL cells showed no measurable heme defects (Supplementary Fig. 4). This indicates that Atpif1 is essential for terminal erythroid maturation and is not critical for heme synthesis in non-erythroid cells and early erythroid progenitors.

Under physiological conditions, the F<sub>1</sub>F<sub>0</sub>-ATP synthase generates a proton motive force and ATP by transporting H<sup>+</sup> ions into the mitochondria<sup>8, 15</sup>. Under oxidative stress, the F<sub>1</sub>F<sub>0</sub>-ATP synthase reverses the direction of H<sup>+</sup> transport, thus reducing ATP and proton motive force<sup>8, 15</sup>. Atpif1 inhibits the reversal of F<sub>1</sub>F<sub>0</sub>-ATP synthase to reduce ATP hydrolysis, thereby maintaining the mitochondrial membrane potential and proton motive force<sup>8</sup>. To determine the causal association between the roles of Atpif1 in mitochondrial homeostasis and mammalian heme synthesis, we used stable *Atpif1*-shRNA-silenced MEL cells. Consistent with the silencing of *Atpif1*, the Atpif1 protein levels were reduced (Fig. 3b). While excluding the possibility of global mitochondrial structural dysfunction: (1) We found normal protein expression of integral mitochondrial proteins, such as the  $\beta$ -subunit of ATP synthase (AtpB), complex IV (Cox IV), voltage-dependent anionic-selective channel protein 1 (Vdac1), and heat shock protein 60 (Hsp60) (Fig. 3b). (2) Electron microscopic and biochemical analysis revealed normal integrity of the mitochondria; indicating that the gross structural architecture of mitochondria in *Atpif1*-silenced MEL cells was preserved (Fig. 3b, Supplementary Fig. 5). We, however, found that the loss of *Atpif1* in differentiating MEL cells caused a depletion of cellular ATP levels (Supplementary Figs. 6a–6b), an increase in mitochondrial membrane potential ( $\Delta\Psi_m$ ) (Fig. 3c, Supplementary Fig. 6c), and an alkalization of the mitochondria (Supplementary Fig. 6d).

Heme synthesis requires the incorporation of ferrous ion (Fe<sup>2+</sup>) into protoporphyrin IX (PPIX), which is catalyzed by Fech on the matrix side of the inner mitochondrial membrane<sup>16</sup>. Since the loss of *Atpif1* results primarily in a defect of heme synthesis in differentiating erythroid cells, we analyzed the mitochondrial levels of heme substrates, heme, and their enzymes. We have previously shown that *Mfn1*, an inner mitochondrial membrane transporter, facilitates the import of Fe into erythroid mitochondria<sup>10</sup>; which is dependent upon the mitochondrial  $\Delta\Psi_m$ <sup>17,18</sup>. Consistent with the increased mitochondrial  $\Delta\Psi_m$  in *Atpif1*-silenced MEL cells (Fig. 3c, Supplementary Fig. 6c), the uptake of radio-labeled iron (<sup>59</sup>Fe) into the mitochondria was increased (Fig. 3d), indicating that the loss of *Atpif1* increases mitochondrial iron load. Iron transported into the mitochondrial matrix is either: 1) utilized to make [2Fe-2S] clusters, or 2) incorporated into PPIX by Fech to generate heme<sup>1, 2, 3, 13</sup>. *Atpif1*-silenced MEL cells had normal levels of mitochondrial PPIX (Fig. 3e), suggesting that enzymes and substrates necessary to make this heme precursor are not rate-limiting. The incorporation of <sup>59</sup>Fe into PPIX to generate heme, however, was reduced (Fig. 3f), despite having sufficient levels of Fech substrates, iron and PPIX. We predicted that the catalytic efficiency of Fech might have been compromised, and thus, we measured the protein expression levels of Fech and Fech activity. Although normal levels of Fech protein were present, Fech activity was reduced (Fig. 4a), suggesting that the defect in heme synthesis in *pnt* could be attributed to a reduction in Fech activity. We found that the basal mitochondrial pH of control cells was pH 7.4, and for *Atpif1*-silenced MEL cells was

pH 8.6 (Fig. 4b, Supplementary Fig. 6d). Since *Atpif1*-silenced MEL cells have higher basal mitochondrial pH, we predicted that (1) elevated mitochondrial pH might influence the efficiency of Fech to make heme, and (2) the Fech isolated from these cells is already harmfully influenced by the elevated pH. To experimentally support our hypothesis, we pre-incubated the purified human Fech at pH 7.4, 8.0, 8.5, and 9.0 for 1 hr, and then run Fech assay at pH 7.4. We found that pre-incubation at elevated pH have harmful impact on human Fech, and thus reduces its capacity to make heme (Supplementary Fig. 6e). In addition, we found that increasing mitochondrial pH to 8.5 and pH 9.0 would further lower Fech activity in both control and *Atpif1*-silenced MEL cells (Fig. 4c), indicating the Fech activity is a function of mitochondrial pH (Supplementary Discussion 3). Altogether, these data suggest that the ability of Fech to generate heme was compromised due to the increase in mitochondrial pH that occurs in *Atpif1*-silenced differentiating MEL cells.

We further found that the lowering mitochondrial membrane potential and thus mitochondrial pH, using pharmacological agents carbonyl cyanide 4-(trifluoromethoxy)phenylhydrazone (FCCP; 1 mM; 1hr) and 2, 4-dinitro-phenol (2,4-DNP; 500  $\mu$ M; 1hr)<sup>19</sup>, could rescue anemic phenotype in *Atpif1*-silenced MEL cells (Fig. 4d). These data reinforce our observation that *Atpif1* regulates heme synthesis via its modulation of the mitochondrial  $\Psi_m$  and mitochondrial pH.

*Atpif1*-silenced MEL cells have normal cytosolic and mitochondrial [2Fe-2S] cluster biogenesis as they have normal activities of proteins dependent on [2Fe-2S] cluster synthesis, such as cytosolic xanthine oxidase (Supplementary Fig. 7a), and mitochondrial aconitase (Fig. 4e). The post-translational stability of Fech apoprotein depends on iron availability and an intact [2Fe-2S] cluster assembly machinery<sup>20, 21</sup>. However, the functional role of the [2Fe-2S] cluster in Fech activity remains unknown (Supplementary Discussion 4). All vertebrate Fech enzymes possess [2Fe-2S] clusters, whereas Fech from the yeast *Saccharomyces cerevisiae* does not have a cluster<sup>16, 21</sup>. Based on these data and our current observations, we hypothesized that the [2Fe-2S] cluster of Fech could influence Fech activity *in situ* by rendering Fech responsive to changes in the mitochondrial proton motive force, and thus mitochondrial pH and redox potential.

To experimentally test whether [2Fe-2S] cluster-bound Fech responded to the capacity of *Atpif1* to regulate mitochondrial proton motive force and thus mitochondrial pH, we designed constructs containing either zebrafish Fech (with [2Fe-2S]) or yeast Fech (without [2Fe-2S]) with the vertebrate mitochondrial targeting pro-peptide for cRNA injections. Both constructs, irrespective of the presence of [2Fe-2S] clusters, functionally complemented a genetic deficiency for zebrafish Fech in *freixene*<sup>6, 22</sup> (*frx<sup>tu271</sup>*, Supplementary Fig. 7b). When either zebrafish Fech or yeast Fech cRNA was injected into *pnt* embryos, the yeast Fech rescued *pnt* anemia, while zebrafish Fech did not (Fig. 4f). These data suggest that it is the [2Fe-2S] cluster of the zebrafish Fech that makes this enzyme vulnerable to pH perturbations of the mitochondrial matrix in *atpif1*-deficient *pnt* embryos. Therefore, *Atpif1* plays an essential role in stabilizing the activity of [2Fe-2S] cluster-containing Fech by modulating changes in mitochondrial matrix pH. Based upon our results, we infer that yeast Fech, lacking the [2Fe-2S] cluster, is resistant to mitochondrial pH changes in *pnt* embryos. Consistent with our observation that the activity of yeast Fech would be unaffected by mitochondrial pH (Fig. 4f), we found that the deficiency of *Inh1* did not produce a defect in heme synthesis (data not shown). These data show that *Atpif1* regulates heme synthesis in higher vertebrate erythroid tissues, while its counterpart in baker's yeast, *Inh1*, does not regulate heme synthesis.

The redox potential of mitochondrial matrix at pH 7.4 is -280 mV, and it is reduced to -370 mV at pH 8.4<sup>23</sup>. Since the mitochondrial pH is inversely related to mitochondrial redox

potential<sup>23</sup>, we further analyzed the susceptibility of the [2Fe-2S] of Fech to reduction in mitochondrial redox potential. When we treated human Fech (with [2Fe-2S]) and yeast Fech (without [2Fe-2S]) with a strong reducing agent, sodium dithionite (DTN, 10 mM), we found that the DTN treatment could only reduce the activity of human Fech and not the activity of yeast Fech (Fig. 4g). This further suggests that [2Fe-2S] of vertebrate Fech is sensitive to the reduction in the redox potential. Thus, the Fech activity is reduced in *Atpif1*-silenced MEL cells as its [2Fe-2S] cluster is sensitive to an elevation of pH (Fig. 4b, 4c, 4d, 4f) and a reduction in redox potential (Fig. 4g), and not due to a defect in [2Fe-2S] cluster biosynthetic assembly (Fig. 4e, Supplementary Fig. 7a).

To exclude an anemic phenotype in *pnt* as a causal effect of reactive oxygen species (ROS) induced heme degradation, we treated *pnt* mutant embryos with N-acetyl cysteine (NAC, 10  $\mu$ M, 48 hr), a potent antioxidant employed for ROS studies in zebrafish embryos<sup>24, 25</sup>, and found that NAC could not rescue *pnt* anemia (Fig. 4h). This demonstrates that anemic phenotype in *pnt* is not due to increased ROS generation. The heme-oxygenase-1 enzyme (*Hmox1*) is a ROS-responsive, cellular enzyme responsible for heme degradation. We found normal transcript levels of *Hmox1* in control and *Atpif1*-silenced MEL cells (Supplementary Fig. 7c). Consistent with our model, it has been demonstrated that 1) only overexpression of *Atpif1*, not loss of *Atpif1* activity, induces ROS production, independent of the *Hif1 $\alpha$*  pathway<sup>26</sup>, and 2) the overexpression of *Atpif1* did not affect cellular hydrogen peroxide levels, indicating that the *Atpif1*-mediated superoxide signal is of mild-intensity and localized in mitochondria<sup>26</sup>. Altogether, these data suggest that ROS and heme degradation are not responsible for the heme defect we observed in erythroid cells.

In summary, *Atpif1* modulates the mitochondrial pH and redox potential, and thus allows Fech to efficiently catalyze the incorporation of iron into PPIX to produce heme. Loss of *Atpif1* allows the mitochondrial pH and, consequently, the redox potential to change to a level that reduces [2Fe-2S] cluster-containing Fech activity, thereby reducing heme synthesis, resulting in hypochromic anemia in *pnt* (Fig. 4i). Previous human studies have identified *ALAS2*, *FXN*, *ABCB7*, and *SLC25A38* as the genetic causes of congenital sideroblastic anemias<sup>27, 28</sup>. Data presented herein demonstrate that *Atpif1* should now be added to the list of proteins whose native function is required for normal erythropoiesis. This makes *Atpif1* a candidate gene for the understanding and treatment of human sideroblastic anemias and mitochondrial disorders.

## METHODS SUMMARY

All procedures were approved by the Animal Care and Use Committee of Boston Children's Hospital. We performed complete blood count and Wright-Geimsa analyses on peripheral blood recovered from adult *pnt*. Genetic mapping and positional cloning were utilized to identify *zgc: 162207 (atpif1a)* as the candidate gene for the *pnt* locus on zebrafish Chr. 19. We employed qRT-PCR using TaqMan gene expression assays (Applied Biosystems, Carlsbad, CA) to measure levels of *atpif1a* and *atpif1b* mRNA. Morpholinos (Gene Tools, Philomath, OR) against splice-site of *atpif1a* and *atpif1b* were designed and injected in WT embryos to verify loss-of-function phenotype. The cRNA for *atpif1a*, *atpif1a*-E26A, and *atpif1b* were injected in *pnt* embryos for complementation. The cDNA prepared from WT and *pnt* embryos was sequenced, and the polymorphism in the 3' UTR of the *atpif1a* sequence was verified using SSCP gels.

We silenced *Atpif1* in hCD34+, MPFL and MEL using shRNAs. The *Atpif1*-silenced, differentiated hCD34+ and MEL cells were stained with  $\alpha$ -dianisidine to measure hemoglobinized cells, while MPFL cells were treated with Drabkin's reagent to measure relative hemoglobin content. The loss of *Atpif1* protein and the state of mitochondrial

structural proteins in MEL cells were verified using western and electron microscopic analyses. We analyzed fluorescent intensities of TMRE as a function of mitochondrial membrane potential, Mg green as a function of ATP levels, and ratio of carboxy SNARF-1 to Mitotracker green as a function of the mitochondrial matrix pH<sup>8, 12</sup>.

We prepared <sup>59</sup>Fe-saturated transferrin, and measured <sup>59</sup>Fe incorporated in mitochondria and complexed in heme using a gamma counter. We examined PPIX levels and the catalytic efficiency of FeCh in MEL cells using spectrophotometric analysis. The MEL cells were treated with FCCP and 2,4-DNP, followed by analysis for hemoglobinized cells. Human and yeast FeCh were treated with DTN, and subsequently their catalytic efficiency were measured. Aconitase activity was determined as a measure of [2Fe-2S] cluster levels<sup>29</sup>. The cRNA for zebrafish FeCh or yeast FeCh was injected in *pnt* embryos, and their efficiency to rescue the anemia in *pnt* was measured using *o*-dianisidine staining and verified by using SSCP analysis<sup>10</sup>. Statistical analyses were performed by paired or un-paired t-test. Significance was set at p<0.05.

## Supplementary Material

Refer to Web version on PubMed Central for supplementary material.

## Acknowledgments

We thank members of our lab (Michelle Cassim, Adam Kaplan, Gordon Hildick-Smith, and Heidi Anderson) and colleagues (Seth L. Alper, Karen Pepper, and Nikolaus S. Trede) for critical review of the manuscript, Terrence C. Law for *pnt* adult blood characterization, Howard Mulhern for help with the electron microscopy, Christopher Lawrence and his team for the zebrafish husbandry. This research was supported in part by the Cooley's Anemia Foundation (D.I.S., C.C.), the March of Dimes Foundation (B.H.P.), the American Heart Association (J.D.C., A.E.M.), the Dutch National Science Fund (I.J.S.), the *Fondation Soldati pour la Recherche en Cancerologie* (G.V.), the Burroughs Wellcome Fund (N.N.D.), the NIDDK (D.I.S., B.H.P., A.N., J.K., H.A.D., S.M.H.), and the NHLBI (D.I.S., B.H.P.).

## References

- Schultz IJ, Chen C, Paw BH, Hamza I. Iron and porphyrin trafficking in heme biogenesis. *J Biol Chem.* 2010; 285:26753–9. [PubMed: 20522548]
- Iolascon A, De Falco L, Beaumont C. Molecular basis of inherited microcytic anemia due to defects in iron acquisition or heme synthesis. *Haematologica.* 2009; 94:395–408. [PubMed: 19181781]
- Severance S, Hamza I. Trafficking of heme and porphyrins in metazoa. *Chem Rev.* 2009; 109:4596–616. [PubMed: 19764719]
- Anderson, KE.; Sassa, S.; Bishop, DF.; Desnick, RJ. The Online Metabolic & Molecular Basis of Inherited Disease. Bishop, DF., editor. The McGraw-Hill Press; New York, NY: 2011. p. 1-153.
- Shin JT, Fishman MC. From Zebrafish to human: modular medical models. *Annu Rev Genomics Hum Genet.* 2002; 3:311–40. [PubMed: 12142362]
- Ransom DG, et al. Characterization of zebrafish mutants with defects in embryonic hematopoiesis. *Development.* 1996; 123:311–9. [PubMed: 9007251]
- Postlethwait JH, et al. Vertebrate genome evolution and the zebrafish gene map. *Nat Genet.* 1998; 18:345–9. [PubMed: 9537416]
- Campanella M, Parker N, Tan CH, Hall AM, Duchon MR. IF(1): setting the pace of the F(1)F(o)-ATP synthase. *Trends Biochem Sci.* 2009; 34:343–50. [PubMed: 19559621]
- Ando C, Ichikawa N. Glutamic acid in the inhibitory site of mitochondrial ATPase inhibitor, IF(1), participates in pH sensing in both mammals and yeast. *J Biochem.* 2008; 144:547–53. [PubMed: 18687699]
- Shaw GC, et al. Mitoferrin is essential for erythroid iron assimilation. *Nature.* 2006; 440:96–100. [PubMed: 16511496]



11. Houseley J, Tollervey D. The many pathways of RNA degradation. *Cell*. 2009; 136:763–76. [PubMed: 19239894]
12. Campanella M, et al. Regulation of mitochondrial structure and function by the F1Fo-ATPase inhibitor protein, IF1. *Cell Metab*. 2008; 8:13–25. [PubMed: 18590689]
13. Richardson DR, et al. Mitochondrial iron trafficking and the integration of iron metabolism between the mitochondrion and cytosol. *Proc Natl Acad Sci U S A*. 2010; 107:10775–82.
14. Nilsson R, et al. Discovery of genes essential for heme biosynthesis through large-scale gene expression analysis. *Cell Metab*. 2009; 10:119–30. [PubMed: 19656490]
15. Walker JE. The regulation of catalysis in ATP synthase. *Curr Opin Struct Biol*. 1994; 4:912–8. [PubMed: 7712295]
16. Lanzilotta, WN.; Dailey, HA. Human ferrochelatase in *Handbook of Metalloproteins*. Messerschmidt, A., editor. Vol. 4&5. John Wiley & Sons, Ltd; Chichester, UK: 2011. p. 138-146.
17. Lange H, Kisfalvi G, Lill R. Mechanism of iron transport to the site of heme synthesis inside yeast mitochondria. *J Biol Chem*. 1999; 274:18989–96. [PubMed: 10383398]
18. Froschauer EM, Schweyen RJ, Wiesenberger G. The yeast mitochondrial carrier proteins Mrs3p/Mrs4p mediate iron transport across the inner mitochondrial membrane. *Biochim Biophys Acta*. 2009; 1788:1044–50. [PubMed: 19285482]
19. Park D, et al. Continued clearance of apoptotic cells critically depends on the phagocyte Ucp2 protein. *Nature*. 2011; 477:220–4. [PubMed: 21857682]
20. Crooks DR, Ghosh MC, Haller RG, Tong WH, Rouault TA. Posttranslational stability of the heme biosynthetic enzyme ferrochelatase is dependent on iron availability and intact iron-sulfur cluster assembly machinery. *Blood*. 2010; 115:860–9. [PubMed: 19965627]
21. Medlock AE, Dailey HA. Examination of the activity of carboxyl-terminal chimeric constructs of human and yeast ferrochelatases. *Biochemistry*. 2000; 39:7461–7. [PubMed: 10858295]
22. Childs S, et al. Zebrafish dracula encodes ferrochelatase and its mutation provides a model for erythropoietic protoporphyria. *Curr Biol*. 2000; 10:1001–4. [PubMed: 10985389]
23. Hu J, Dong L, Outten CE. The redox environment in the mitochondrial intermembrane space is maintained separately from the cytosol and matrix. *J Biol Chem*. 2008; 283:29126–34. [PubMed: 18708636]
24. Yu D, et al. miR-451 protects against erythroid oxidant stress by repressing 14-3-3zeta. *Genes Dev*. 2010; 24:1620–33. [PubMed: 20679398]
25. North TE, et al. PGE2-regulated wnt signaling and N-acetylcysteine are synergistically hepatoprotective in zebrafish acetaminophen injury. *Proc Natl Acad Sci U S A*. 2010; 107:17315–20. [PubMed: 20855591]
26. Formentini L, Sanchez-Arago M, Sanchez-Cenizo L, Cuezva JM. The Mitochondrial ATPase Inhibitory Factor 1 Triggers a ROS-Mediated Retrograde Prosurvival and Proliferative Response. *Mol Cell*. 2012; 45:731–42. [PubMed: 22342343]
27. Sheftel AD, Richardson DR, Prchal J, Ponka P. Mitochondrial iron metabolism and sideroblastic anemia. *Acta Haematol*. 2009; 122:120–33. [PubMed: 19907149]
28. Camaschella C. Hereditary sideroblastic anemias: pathophysiology, diagnosis, and treatment. *Semin Hematol*. 2009; 46:371–7. [PubMed: 19786205]
29. Li L, Kaplan J. A mitochondrial-vacuolar signaling pathway in yeast that affects iron and copper metabolism. *J Biol Chem*. 2004; 279:33653–61. [PubMed: 15161905]

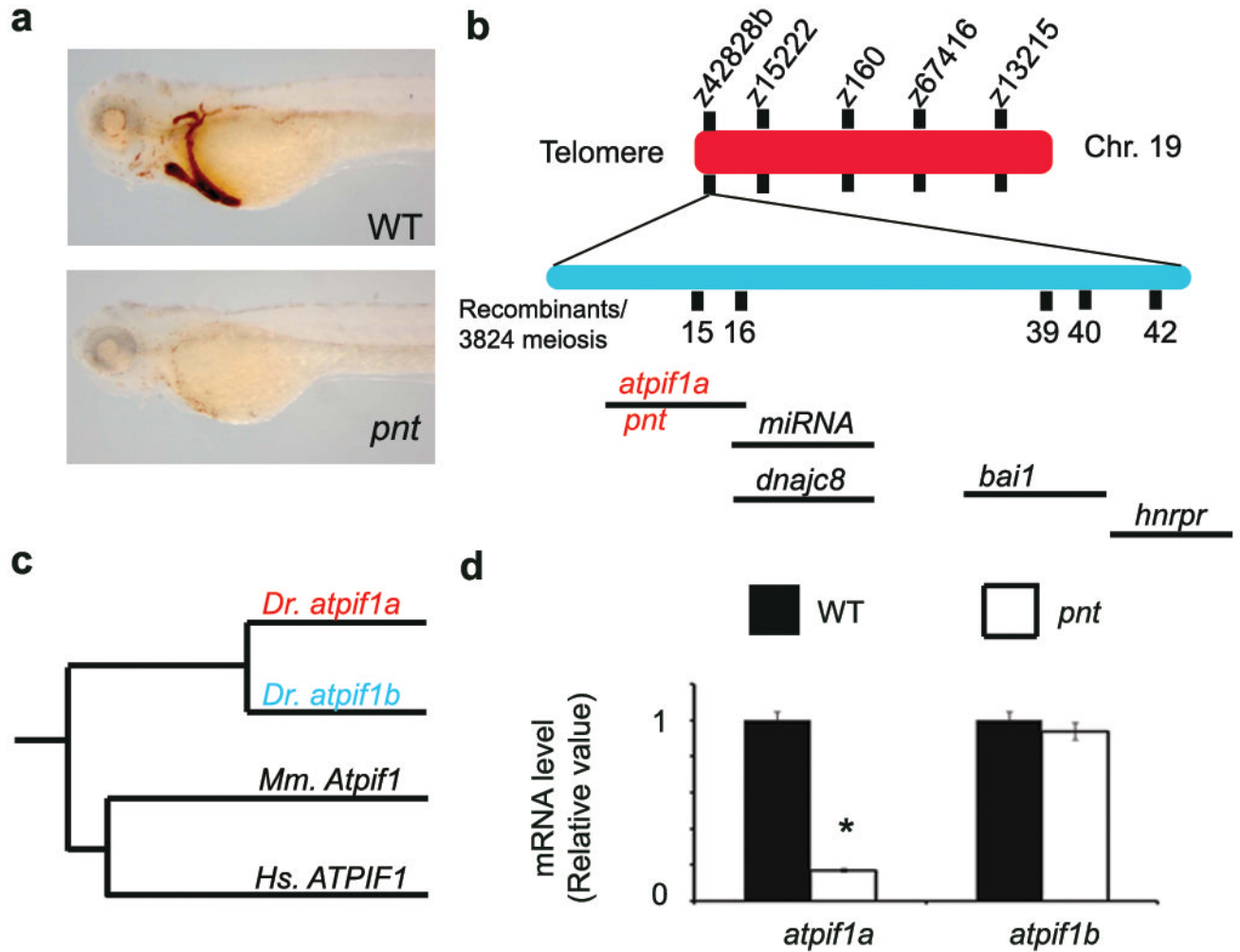


**Fig. 1. Disruption of *atpif1* in pinotage (*pnt*<sup>tq209</sup>) produces hypochromic anemia**  
**a**, *pnt* embryos are severely anemic. Wild-type (WT) embryo at 72 hpf exhibits  $\alpha$ -dianisidine stained (brown) hemoglobinized cells. **b**, The positional cloning of the *pnt* locus on zebrafish chromosome (Chr.) 19. A positional cloning effort with 1,912 diploid *pnt* embryos identified the closest linked genetic marker, z42828b. We initiated a chromosomal walk, at a distance of  $\sim$ 0.01 centimorgan (cM) from the *pnt* locus. The BAC clone, encompassing the *pnt* locus, is shown below, along with the annotated genes within the critical physical contig. **c**, Phylogenetic dendrogram showing the amino acid homology between the various *atpif1* genes. *D. rerio* (*Dr.*) *atpif1a* aligns with its related paralog, *atpif1b*, on zebrafish Chr. 17. Both *atpif1a* and *atpif1b* are shown clustering with their functional mammalian orthologs from mouse (*Mm.*) and human (*Hs.*). **d**, qRT-PCR analysis of *atpif1a* and *atpif1b* mRNA in *pnt* and WT embryos, showing reduced *atpif1a* and normal *atpif1b* mRNA level in *pnt*. \* $p < 0.05$  (t-test,  $n=3$ )

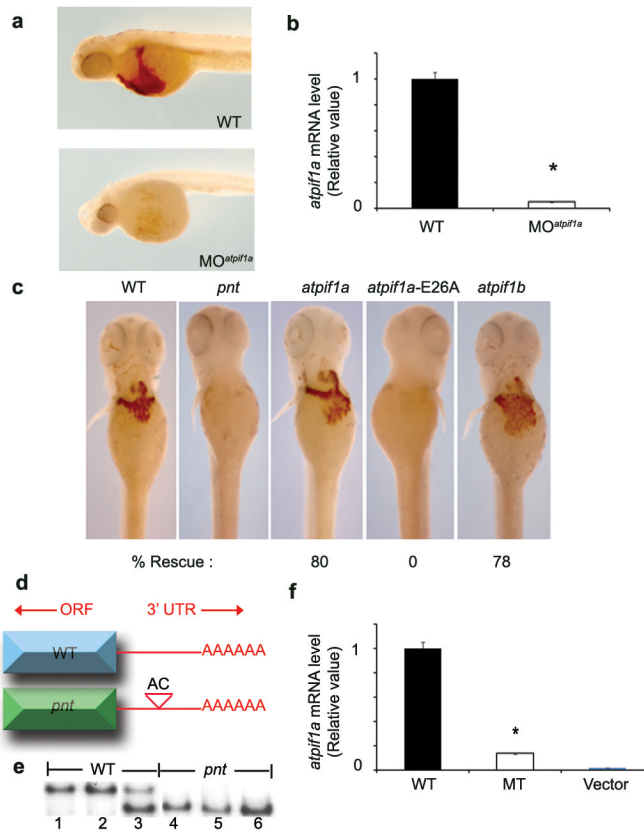


### Fig. 2. Functional characterization of the *atpif1a* gene

**a**, Splice blocking morpholino (MO) knock down of *atpif1a* phenocopies the anemia observed in *pnt* embryos. **b**, qRT-PCR analysis shows that the anemic phenotype is due to the accurate knockdown of *atpif1a*. **c**, Ectopic expression of *atpif1a* or *atpif1b* cRNA functionally complements the anemia in *pnt* embryos at 72 hpf. WT control, *pnt*, and rescued *pnt* embryos complemented with *atpif1a* or *atpif1b* cRNA are stained with *o*-dianisidine. The non-functional *atpif1a*, harboring the E26A mutation, specifically failed to complement the *pnt* anemia. **d**, *pnt* embryos have an AC polymorphism in the 3' UTR of the *atpif1a* gene. **e**, The 3' UTR AC polymorphism co-segregates with the *pnt* phenotype by SSCP analysis. The SSCP segregation pattern for lanes 1–2 (+/+), lane 3 (+/*pnt*), and lanes 4–6 (*pnt/pnt*). **f**, The mutant AC polymorphism in the 3' UTR of the *atpif1a* cDNA functionally destabilizes its mRNA. MT construct stably expressed in MEL cells showed reduced *atpif1a* mRNA levels. \* $p < 0.05$  (t-test,  $n = 3$ )

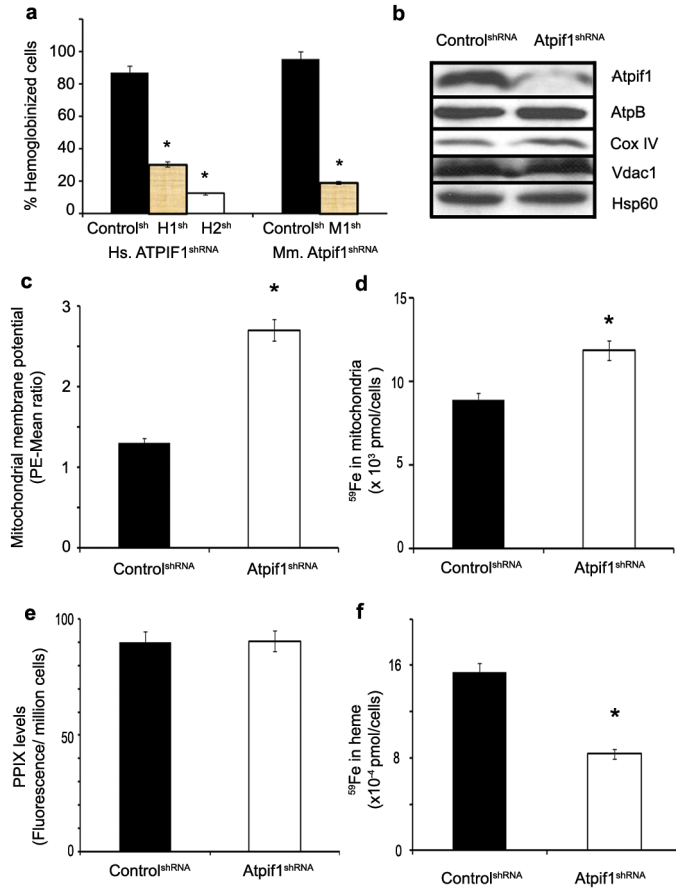


**Fig. 3. Loss of Atpif1 produces a hemoglobinization defect in mammalian cells**

**a**, Silencing of *Atpif1* in human CD34+ (left) and MEL (right) cells with shRNAs (Human: H1<sup>sh</sup> & H2<sup>sh</sup>, Mouse: M1<sup>sh</sup>) results in a hemoglobinization defect. **b**, Western analysis in *Atpif1*-shRNA (Mouse: M1<sup>sh</sup>) silenced MEL cells. *Atpif1* protein level is reduced in *Atpif1*-shRNA (M1<sup>sh</sup>)-silenced cells. However, the mitochondrial structural proteins, AtpB, CoxIV, Vdac1, and Hsp60, are not affected. **c**, Silencing of *Atpif1* elevates the mitochondrial membrane potential ( $\Delta\Psi_m$ ), analyzed using a TMRE fluorescence probe in the presence of verapamil and FCCP. **d**, Silencing of *Atpif1* elevates the import of <sup>59</sup>Fe in the mitochondria, consistent with the increased mitochondrial  $\Delta\Psi_m$ . **e**, Silencing of *Atpif1* does not influence the formation of protoporphyrin IX (PPIX), indicating PPIX and iron are not limited for heme synthesis. **f**, The level of <sup>59</sup>Fe incorporated in heme is greatly reduced in *Atpif1*-silenced MEL cells, recapitulating the heme synthesis defect in *pnt*. \*p<0.05 (t-test, n=3)

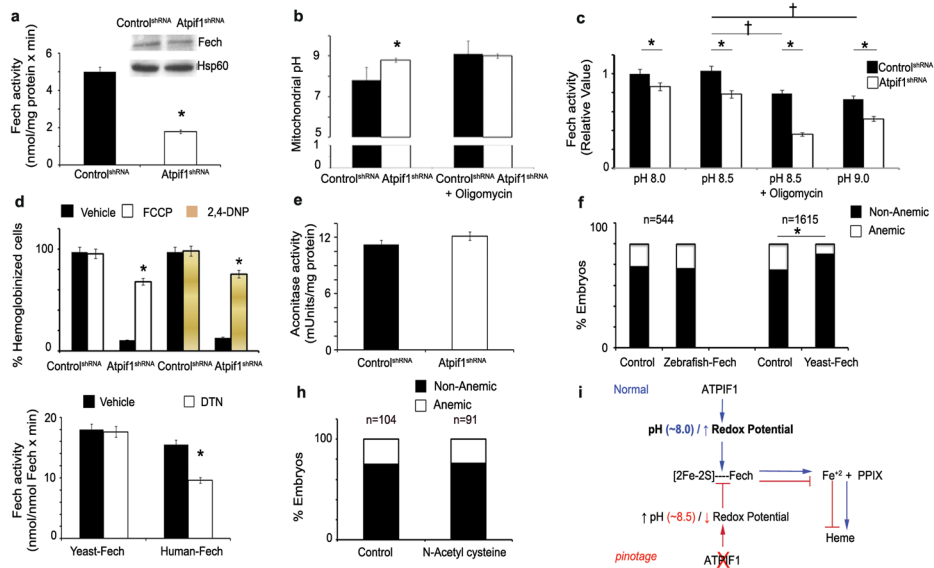


**Fig. 4. Atpif1 regulates heme synthesis by modulating Fech activity**

**a**, Ferrochelatase (Fech) protein levels are normal (top right); however, the Fech activity is reduced in *Atpif1*-silenced MEL cells. **b**, Silencing of *Atpif1* increases the mitochondrial matrix pH to 8.6. The histogram summarizes values at resting conditions and after challenge with oligomycin that normalizes the initial difference. **c**, Analysis of Fech activity as a function of pH. The elevation of mitochondria pH to 8.5 & 9.0 markedly reduced the Fech activity. **d**, Drugs lowering mitochondrial membrane potential reverses the anemic phenotype due to loss of *Atpif1*. Treatment of FCCP and 2, 4-DNP complements the anemic phenotype of *Atpif1*-silenced MEL cells. **e**, Aconitase activity, a marker for mitochondrial [2Fe-2S] cluster synthesis, is normal in *Atpif1*-silenced MEL cells. **f**, The presence of [2Fe-2S] cluster makes Fech susceptible to mitochondrial pH alteration in the absence of *Atpif1*. Yeast Fech, lacking [2Fe-2S], complements *pnt* anemia, indicating a resistance to pH changes in the absence of *atpif1*. Zebrafish Fech, containing [2Fe-2S], does not complement *pnt* anemia, indicating its susceptibility to mitochondrial alkalization. **g**, The [2Fe-2S] of Fech is sensitive to the reduction in redox potential. The treatment of DTN reduces human Fech activity, and does not affect yeast Fech activity. **h**, Reactive oxygen species (ROS) are not responsible for *pnt* anemia. Treatment of *pnt* embryos with N-acetyl cysteine (NAC) does not reverse *pnt* anemia. **i**, A proposed mechanistic model of *Atpif1* function in the maintenance of mitochondrial pH and regulation of Fech activity for heme synthesis. Mitochondrial heme synthesis requires Fech to incorporate iron into PPIX at physiological pH. *Atpif1* normally preserves the mitochondrial pH. Loss of *Atpif1* alkalizes mitochondrial pH, the presence of [2Fe-2S] cluster makes Fech susceptible to mitochondrial pH and redox potential perturbations, and consequently reduces its catalytic efficiency for the production of heme. \* $p < 0.05$  (t-test,  $n=3$ ); † $p < 0.05$  vs. control cells at pH 8.5 (t-test,  $n=3$ )